JACC Vol. 27, No. 5
April 1996:1264–9

In Vitro Flow Experiments for Determination of Optimal Geometry of Total Cavopulmonary Connection for Surgical Repair of Children With Functional Single Ventricle

SHIVA SHARMA, MD, FACC, SEAN GOUDY, BS,* PETER WALKER, PHD,*
SAMIR PANCHAL, MS,* ANN ENSLEY, BS,* KIRK KANTER, MD,† VINCENT TAM, MD,†
DEREK FYFE, MD, PHD, AJIT YOGANATHAN, PHD*

Atlanta, Georgia

Objectives. **This study sought to evaluate the effect of offsetting cavopulmonary connections at varying pulmonary flow ratios to determine the optimal geometry of the connection.**

Background. **Previous investigators have demonstrated energy conservation within the streamlined contours of the total cavopulmonary connection compared with that of the atriopulmonary connection. However, their surgical design of connecting the two cavae directly opposite each other may result in high energy losses. Others have introduced a unidirectional connection with some advantages but with concerns about the formation of arteriovenous malformation in the lung excluded from hepatic venous return. Thus, an optimal surgical design has not been determined.**

Methods. **In the present models, the caval connections were offset through a range of 0.0 to 2.0 diameters by 0.5 superior cava diameter increments. Flow ratios were fixed for superior and inferior cavae and varied for right and left pulmonary arteries as 70:30, 60:40, 50:50, 40:60 and 30:70 to stimulate varying lung resistance. Pressure measurements and flow visualization were done at steady flows of 2, 4 and 6 liters/min to simulate rest and exercise.**

Results. **Our data show that the energy losses at the 0.0-diameter offset were double the losses of the 1.0 and 1.5 diameters, which had minimal energy losses. This result was attributable to chaotic patterns seen on flow visualization in the 0.0-diameter offset. Energy savings were more evident at the 50:50 right/left pulmonary artery ratio. Energy losses increased with increased total flow rates.**

Conclusions. **The results strongly suggest the incorporation of caval offsets in future total cavopulmonary connections.**

(J Am Coll Cardiol 1996;27:1264–9)

The history of surgical management of patients with a functional single ventricle has been characterized by modifications, many of which were done to reduce complications and improve the functional outcome of children (1–3). One of the major modifications followed the pioneering work of de Leval et al. (4), who demonstrated that pulsatile valveless cavities like the right atrium and venous connections at sharp angles contributed to energy losses. Concomitantly they developed the total cavopulmonary connection with anastomosis of the inferior and superior cava directly opposite each other on the right pulmonary artery (i.e., with zero offset of cavae from each other). A subsequent study (5) comparing the traditional Fontan atriopulmonary connection with the total cavopulmonary connection demonstrated lower systemic venous pressures and a lower incidence of atrial arrhythmia in the latter group of patients. The total cavopulmonary connection concept was extended further by Laks et al. (6) by development of the unidirectional cavopulmonary connection in which the superior vena cava and inferior vena cava were connected exclusively to the left and right pulmonary arteries, respectively, with creation of a fenestration in the inferior channel. The theoretic advantages of this modification were that it provided even lower inferior vena caval pressures and obligatory superior vena caval flow to the left lung. It also matched the relatively higher inferior vena caval flow to the larger volume of the right lung.

Despite these improvements, concerns remain about both these designs. In the zero-offset design, dissipative energy losses are believed to be high at the site of collision of the caval flows. In the unidirectional connection, hepatic venous blood is completely excluded from the left lung by design. Srivastava et al. (7) reported the development of pulmonary arteriovenous malformation in the lung sequestered from hepatic venous blood in their patients with cavopulmonary connections, underscoring the need for hepatic venous perfusion to both lungs. Furthermore, the unidirectional design does not allow for variations in pulmonary resistance to adjust pulmonary blood

From the Children's Heart Center, Emory University School of Medicine; *Cardiovascular Fluid Mechanics Laboratory, Georgia Institute of Technology, School of Chemical Engineering; and †Egleston Children's Hospital at Emory University, Atlanta, Georgia. Sean Goudy was supported by a National Science Foundation Fellowship, Washington, D.C.

Manuscript received June 22, 1995; revised manuscript received November 10, 1995, accepted November 22, 1995.

Address for correspondence: Dr. Shiva Sharma, The Children's Heart Center, 2040 Ridgewood Drive NE, Atlanta, Georgia 30322.

0735-1097/96/$15.00
SSDI 0735-1097(95)00598-6

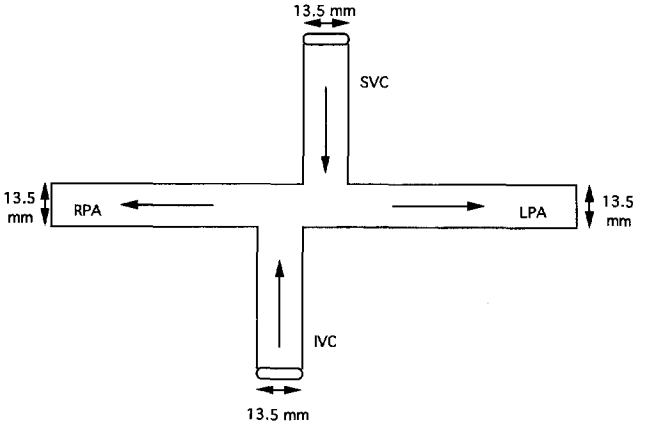

Figure 1. Schematic of 1.0-diameter offset model showing dimensions used. IVC = inferior vena cava; LPA = left pulmonary artery; RPA = right pulmonary artery; SVC = superior vena cava.

flow between the two lungs. Therefore, while allowing for circulatory mixing of systemic venous return, we studied the effects of varying caval offsets at various right and left pulmonary artery flow ratios (varying pulmonary resistance) to determine the optimal combination for minimizing energy losses.

Methods

Determination of glass model sizes. To obtain realistic sizes of the inferior and superior vena cavae and right and left pulmonary arteries, an 8-year old boy with a Fontan operation underwent magnetic resonance imaging (MRI) with a Philips Medical Systems ACS 1.5-tesla scanner. The magnetic resonance images were then transferred to an ISG allegro graphics workstation for image segmentation and three-dimensional reconstruction. From the computer reconstruction, the sizes of inferior and superior vena cavae and right and left pulmonary arteries were measured.

Experimental system and conditions. Figure 1 represents the configuration and dimensions of the 19-mm (1.0-diameter offset) model that was made of custom-crafted Pyrex glass. All inlet and outlet ducts had an inner diameter of 13.5 mm and were ~15 cm long. Five models were constructed with offsets of 0.0 mm (0.0-diameter offset), 8 mm (0.5-diameter offset), 19 mm (1.0-diameter offset), 25 mm (1.5-diameter offset) and 30 mm (2.0-diameter offset). *Offset* was defined as the horizontal distance between the caval midpoints (Fig. 1). A 2-mm diameter hole was drilled into each inlet and outlet conduit to measure the differential static pressure decrease within the models. The holes were used to insert flat-tipped metal catheters that were connected to a pressure transducer. The flow ratios for the superior and inferior cavae were fixed at 40:60, respectively, which was used to reflect the higher superior vena caval flow seen in infants and young children (8,9). The flow ratios to the right and left pulmonary arteries were varied as follows: 30:70, 40:60, 50:50, 60:40 and 70:30. Pressure measurements were carried out at 2, 4, and 6 liters/min. An aqueous solution of glycerin with a mean (±SD) kinematic viscosity of 3.5 ± 0.1 centistokes was used to reproduce the kinematic viscosity of blood. The viscosity was measured at all stages of data collection to ensure that it remained constant.

By maintaining a constant head differential between the supply and dump tanks, steady flow was produced. We used three rotameters to measure the flow: one measured the total flow; another measured inferior caval flow; the last measured the higher flow of either the right or left pulmonary artery. A multiple-range DP15TL Validyne pressure transducer with a no. 24 diaphragm was used to measure the pressure decrease across each model, using the inferior vena caval inlet as the reference point for each measurement. We collected data for 10 s and averaged these data to get a single mean value for the static pressure decrease.

Flow visualization. To visualize flow through the glass models, neutrally buoyant spherical 100-μm Amberlite particles were added to the water/glycerin solution and illuminated with white light. The experimental flow conditions were the same as those described for pressure measurements. The motion of the particles as they traveled through the models was recorded with a video camera. Flow path lines were obtained by black-and-white photography of the models using a 35-mm camera with 400-ASA speed film with a shutter speed of 1/15 and 1/30 s.

Data analysis. After collecting static pressure ($P_{i,s}$) at each of the conduit measurement ports and the associated volumetric flow (Q_i), the data were analyzed to calculate the velocity (u) through each of the conduits and the power losses associated with each total cavopulmonary connection configuration. Using the velocity data and density data (ρ), the dynamic pressure ($P_{i,ke}$) was calculated as follows:

$$P_{i,ke} = 1/2\rho u^2.$$

Next, using the Bernouilli equation, both the rate of kinetic energy losses ($E_{ke,loss}$) and the rate of potential energy losses ($E_{s,loss}$) were calculated:

$$E_{s,loss} = (Q_{ivc}\cdot P_{ivc,s} + Q_{svc}\cdot P_{svc,s}) - (Q_{rpa}\cdot P_{rpa,s} + Q_{lpa}\cdot P_{lpa,s}),$$

$$E_{ke,loss} = (Q_{ivc}\cdot P_{ivc,ke} + Q_{svc}\cdot P_{svc,ke}) - (Q_{rpa}\cdot P_{rpa,ke} + Q_{lpa}\cdot P_{lpa,ke}).$$

Finally, summing the separate contributions of the power losses (rate of energy losses), the total power losses ($E_{total,loss}$) were calculated as follows:

$$E_{total,loss} = E_{ke,loss} + E_{s,loss}.$$

After calculating the total power losses for all cases studied, we identified the nadir of the power losses at 2 liters/min and used that quantity as the reference value. The reference value (X_{ref}) was then used to calculate the relative percent change of all the cases studied:

$$\% \text{ Change} = (X_i - X_{ref})/X_{ref} \times 100\%.$$

JACC Vol. 27, No. 5
April 1996:1264–9

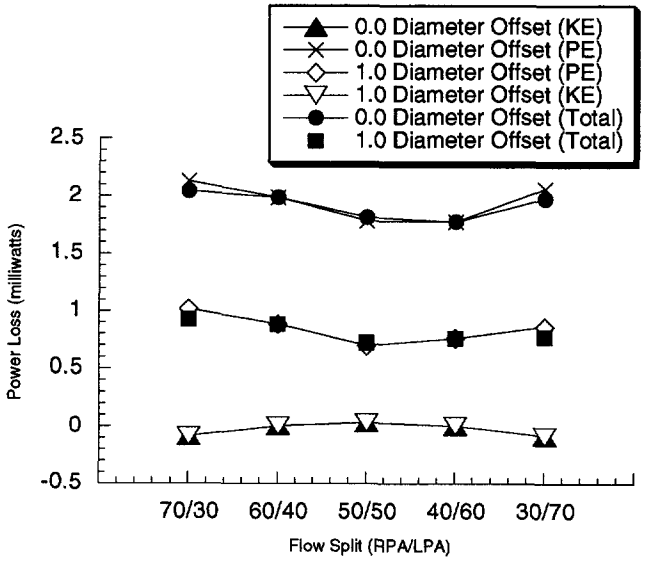

Figure 2. Graph of potential (PE) and kinetic (KE) energy losses for the 0.0- and 1.0-diameter offset at total flow rate of 2 liters/min. Other abbreviations as in Figure 1.

Results

Flow energetics. *Comparison of potential and kinetic energy changes.* Figure 2 shows representative curves of changes in the kinetic, potential and total energy for the 0.0- and 1.0-diameter offset models at 2 liters/min. The net rate of kinetic energy changed only with flow ratio, which affected flow velocity and reached maximal losses at 50:50 right/left pulmonary artery flow ratio. In contrast, the potential energy losses of each of the models varied with offset, flow ratio and flow rate. Comparison of kinetic and potential energy changes, depicted in Figure 2, revealed that the potential energy changes were more than tenfold greater than the kinetic energy changes calculated.

Comparison of total power losses with changes in offset, flow ratio and total flow. Total power losses are summarized in Figure 3, which gives a composite of the total power losses versus offset and flow ratio at 6 liters/min. Figure 3 shows that as the offset was increased from 0.0 to 0.5 superior vena caval diameters, the power losses decreased significantly. When the offset was increased further from 0.5 to 1.0 superior vena caval diameters, there was an additional decrease in the power losses but less marked than the initial decrease. Thereafter, further increases in offset resulted in no significant change in power losses, and the losses for 1.0-, 1.5- and 2.0-diameter offsets did not appear to be significantly different from one another.

Figure 3. Surface plot of power losses versus offset and flow split at 6 liters/min. Abbreviations as in Figure 1.

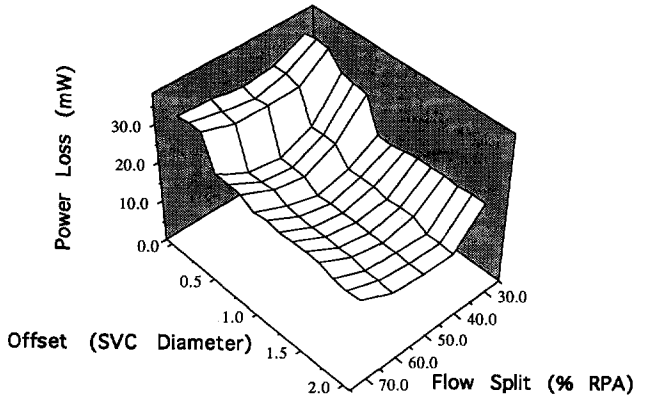

The power losses varied with varying pulmonary flow ratios (Fig. 3 and 4). The power losses were least at the 50:50 flow split, moderate at the 40:60 and 60:40 flow splits and highest at the 30:70 right/left pulmonary artery flow split and the latter change was more obvious at the 0.5-diameter offset.

Figure 4 demonstrates that the power losses were greatly magnified at increased total flow rates. There was a 2,000% increase in power loss in the 1.5-diameter offset from the lowest flow of 2 liters/min to the highest at 6 liters/min, and for the zero offset there was 4,200% increase for a similar increase in total flow.

Flow visualization. Figure 5 demonstrates the effect of offset at a constant flow split for the 60:40 right/left pulmonary artery case. The zero-diameter offset case (Fig. 5, top) demonstrates that the relatively parallel path lines of flow in the two cavae turned into a disorganized pattern of path lines at the site of collision of flow. The 0.5-diameter offset case (Fig. 5, middle) demonstrates a vigorous vortex at the offset site of the cavae. The vortex appears to cushion the caval flows so that there is a bend in superior vena caval flow toward the left pulmonary artery and a slight bend in inferior vena caval flow toward the right pulmonary artery. The higher offsets also demonstrated a vortex, but it was less well defined and less vigorous than the 0.5-diameter offset (1.0-diameter offset [Fig. 5, bottom]). Other than the difference in the vortex, the flow path lines from the 0.5- to 2.0-diameter offsets appeared similar. Downstream pathlines in both pulmonary arteries had helical secondary flow patterns for all offsets.

Figure 6 demonstrates the effects of flow splits at a constant 1.5-diameter offset. The 70:30 right/left pulmonary artery case (Fig. 6, top) demonstrates that the parallel path lines of flow in the superior vena cava collide with the conduit wall and split toward the left and right pulmonary arteries, and the path lines of the inferior vena cava appear to be directed toward the right pulmonary artery. The 30:70 case (Fig. 6, middle) demonstrates that the inferior vena caval flow splits toward left and right pulmonary arteries, whereas the superior vena caval flow appears to bend toward the left pulmonary artery only. In the 50:50 flow split (Fig. 6, bottom), the superior vena caval path lines appear to bend toward the left pulmonary artery, and the inferior vena caval path lines collide with the conduit wall and split, with the larger component going toward the right pulmonary artery and the smaller component toward the left pulmonary artery. The flow path lines for the 40:60 right/left pulmonary artery flow split were similar to those for the 50:50 flow split.

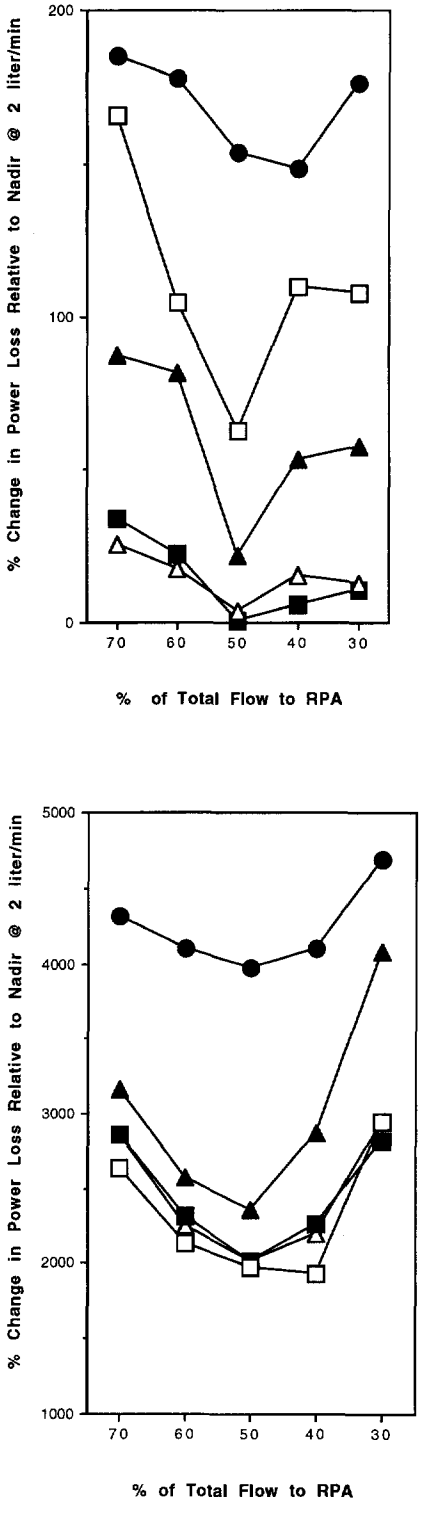

Figure 4. Percent difference in energy loss at 2 (**top**) and 6 liters/min (**bottom**) relative to the nadir at 2 liters/min. **Circles** = 0.0-diameter offset; **solid triangles** = 0.5-diameter offset; **solid squares** = 1.0-diameter offset; **open triangles** = 1.5-diameter offset; **open squares** = 2.0-diameter offset.

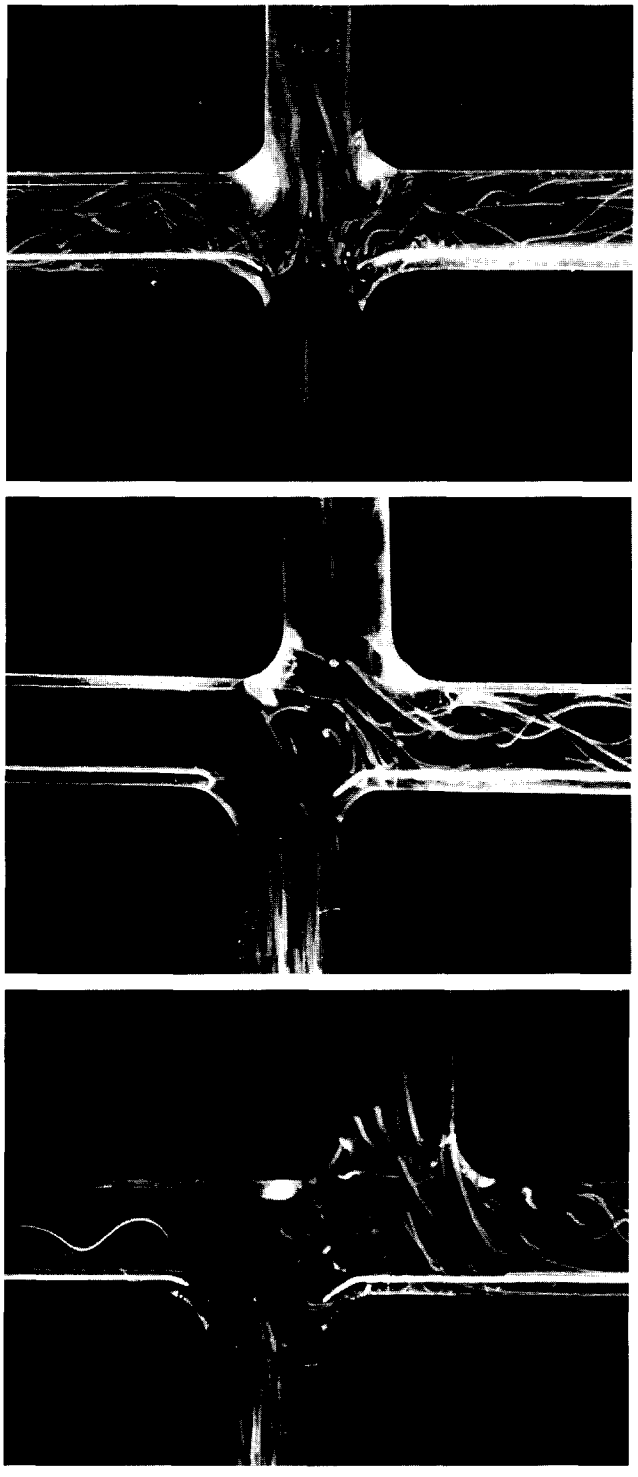

Figure 5. Still photographs of representative models at 60:40 right/left pulmonary artery ratio for 0.0- (**top**), 0.5- (**middle**) and 1.0-diameter offset (**bottom**).

Discussion

When the importance of conserving energy in a single-ventricle supported circulation was realized, recent modifications of the Fontan operation focused on streamlining flow through the connections. In vitro experimental work by de Leval et al. (4) has contributed significantly to the devising of these modifications. Our previous in vitro work (10) pointed out the areas of energy loss in atriopulmonary connections. In the present report we describe our experimental work in

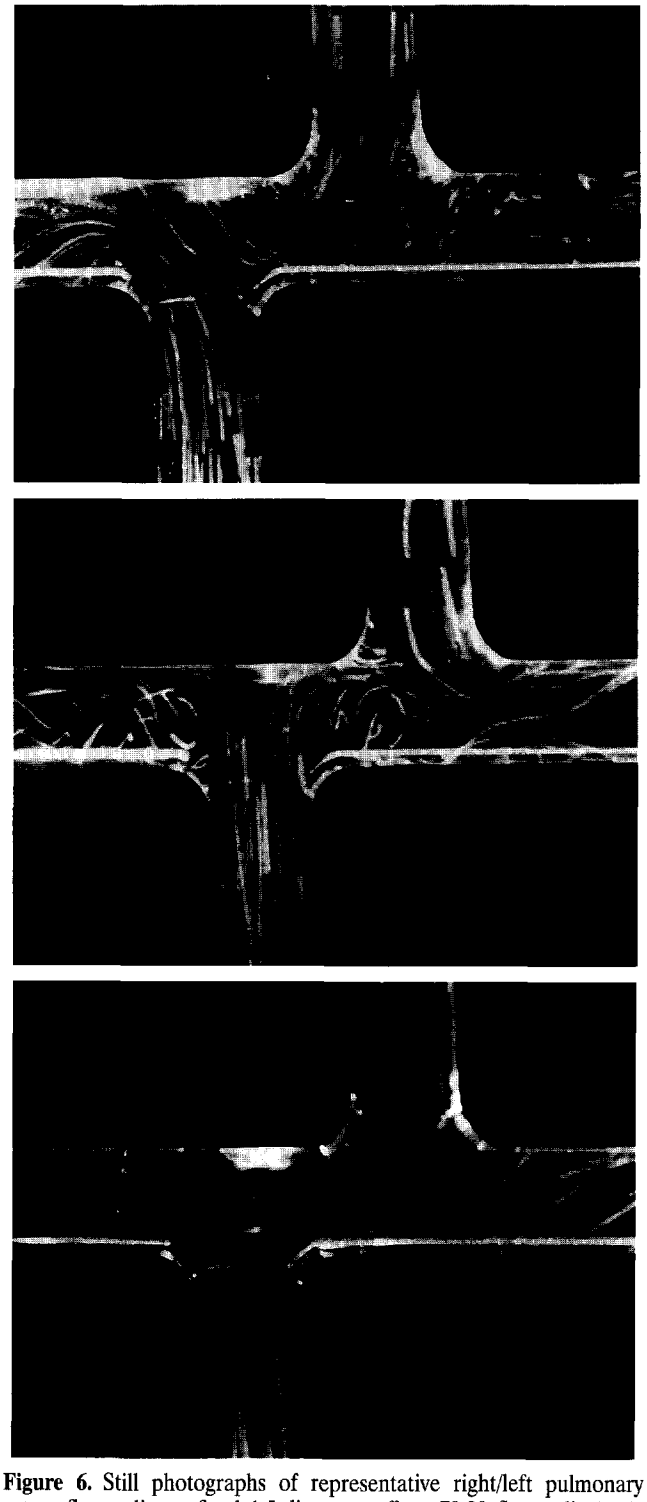

Figure 6. Still photographs of representative right/left pulmonary artery flow splits at fixed 1.5-diameter offset: 70:30 flow split (**top**), 30:70 flow split (**middle**) and 50:50 flow split (**bottom**).

determining the optimal geometry of total cavopulmonary connection that would keep energy losses to a minimum. The study utilized patient-derived sizes of glass models and realistic flow rates found in children. The quantitative portion of our work was supported by extensive flow visualization studies.

Relation between flow energetics and flow visualization. *Effect of offset.* The present study demonstrated that the introduction of caval offsets significantly reduced energy consumption within the connections. At the 0.0-diameter offset, flow visualization demonstrated that the high energy losses measured were due to intensely disorganized flow patterns and secondary flows. At the 0.5-diameter offset, energy losses were ~40% lower than that at the 0.0-diameter offset at 6 liters/min. This finding is confirmed by the flow visualization, which revealed that the vortex at the site of the anastomosis at the 0.5-diameter offset effectively cushioned the collision of the converging caval flows and reduced their interaction and, thus, power losses (Fig. 5, top and middle). Further, at the 1.0- and 1.5-diameter offset, the energy losses were ~50% lower than that at the 0.0-offset at 6 liters/min (Fig. 3). We believe that significantly lower energy losses were measured in the 1.0- and 1.5-diameter offsets because of further reduction in caval flow interaction. This interaction was stronger for the 0.5-diameter case and manifested as a more vigorous central vortex than the vortices at the higher offsets. For this reason, the 0.5-diameter offset was not as efficient in minimizing energy losses as the 1.0- or 1.5-diameter offsets.

Effect of flow split. In addition to determining the effect of offset on power losses, the present study evaluated the effect of variable pulmonary flow ratio and its effects on power losses. Our results show that the power losses associated with the respective offsets were lowest when the pulmonary resistance was equally distributed (i.e., 50:50 pulmonary flow ratio, as explained in the Appendix). In addition, our results show that at a pulmonary resistance equivalent to a 60:40 and 40:60 right/left pulmonary artery flow ratio, power losses were comparably low for a given model and total flow rate and were also nearly symmetric (Fig. 4). These experimental results are consistent with theory (see Appendix).

Surgical applications. *Offset.* Although preliminary, our study has potential surgical applications. The study separated the caval offsets with the least energy losses (1.0 and 1.5 diameter) from those with relatively low (0.5 and 2.0 diameter) and high losses (0.0 diameter). These results imply that future surgical designs should definitely have an offset and that the 1.0- or 1.5-diameter offset would be more desirable. However, our surgeons (V.T., K.K.) believe that anatomic space constraints in some situations may allow a maximal offset of only 0.5 mm in diameter. Our results show that in these situations, energy losses would be also lower than at the 0.0-offset case.

Pulmonary flow ratio. The optimal offsets were found to maintain low losses through a range of pulmonary flow ratios, with the nadir at the 50:50 flow ratio. The importance of this finding lies in the fact that many postoperative patients with a total cavopulmonary connection develop atelectasis, diaphragm paralysis or pleural effusions, which can lead to an alteration in pulmonary resistance. Because of the bidirectional option of flow in our proposed design, pulmonary redistribution can occur without significant energy losses.

Total flow. The present experiments were done at varying total flow rates to simulate the rest and activity cardiac output

seen in children. Although the differences between the best and worst cases for energy loss were significant, they were still relatively small at low flow rates of 2 liters/min. When the flow rate was increased to 6 liters/min, these differences increased 20-fold, underscoring the need for offset.

Mixing. The experimental models, by virtue of not being unidirectional, enabled mixing of caval flows. In the 30:70, 40:60 and 50:50 right/left pulmonary artery flow splits, there was clear visualization of inferior caval flow toward both the right and left pulmonary arteries. In the other models, the central vortex appeared to facilitate mixing. The importance of mixing lies in the provision of hepatic venous blood to both lungs. It was convincingly demonstrated by Srivastava et al. (7) that exclusion of hepatic venous blood from a lung can result in the development of pulmonary arteriovenous malformation in that lung. The factors in hepatic venous blood that prevent this complication have not been isolated and therefore cannot be quantified. Nevertheless, future surgical designs should allow at least some mixing to occur, and our experiments suggest that this mixing can occur at most flow splits and offsets.

Conclusions. The present study investigated the effect of caval offset and varying pulmonary vascular resistance and cardiac output on the energy losses associated with the total cavopulmonary connection. These effects were then related to flow visualization. From these investigations our results indicate that an offset should be incorporated into future total cavopulmonary connection designs, and the ideal offset should be 1.0 to 1.5 mm in diameter. These offsets consume the least amount of energy when vascular resistance is equally distributed between both lungs. Furthermore, increases in cardiac output are associated with increased energy consumption. Our future work will investigate the effect of both curvature and pulsatility on the energy losses associated with the total cavopulmonary connection.

We acknowledge the secretarial help of Ellen Troutman and Leigh Swisher, The Children's Heart Center, Atlanta, Georgia.

Appendix

Theoretical Analysis

It can be shown by the Poiseuille and Bernouilli equations that our experimental results are consistent with previously accepted theories. The Poiseuille equation relates the change in static pressure to the volumetric flow rate:

$$Q = \beta \cdot \Delta P_s,$$

where $\beta = \rho d^4/(128\mu\ \Delta L)$; ΔP_s = change in static pressure; d = diameter; μ = viscosity; and ΔL = change in length; Q = volumetric flow rate.

Figure 2 of our results shows the change in kinetic and potential energy losses versus flow ratio for several representative curves. Moreover, Figure 2 shows that the magnitude of the kinetic power losses are much smaller than the magnitude of the potential power losses. The kinetic and potential power losses are the change in the dynamic and static pressures, respectively, multiplied by the volumetric flow rate:

$$P_{s,loss} = Q \times \Delta P_s, \qquad P_{ke,loss} = Q \times \Delta P_{ke}.$$

If we assume that the dynamic pressure is much smaller than the static pressure terms, we can make the assumption that the change in total pressure is approximately equal to the change in static pressure.

$$\Delta P = \Delta P_{ke} + \Delta P_s, \qquad \Delta P_{total} \approx \Delta P_s.$$

Furthermore, if the change in static pressure is approximately equal to the total pressure, we can substitute the static pressure into the Bernouilli equation for the change in total pressure:

$$\Delta E = Q \times \Delta P_{total}, \qquad \Delta E \approx Q \times \Delta P_s,$$

where E = total power. Finally, if we solve the Poiseuille equation for the change in static pressure and substitute the resultant equation into the Bernouilli equation for the change in static pressure, the resultant equation reveals that the change in power losses are proportional to the square of the volumetric flow rate:

$$\Delta P_s = (1/\beta) \cdot Q, \Delta E \approx Q^2/\beta.$$

In our system we set the input energy by setting the input flow rate for a given total flow (i.e., the superior and inferior vena caval flow rates are set at 40% and 60% of the total flow, respectively). Finally, using the previous truncated equation, when the energy losses associated with each of the respective offsets are calculated, the 50:50 flow ratio consumes less energy regardless of the offset of the models.

References

1. Fontan F, Baudet E. Surgical repair of tricuspid atresia. Thorax 1971;26: 240–8.
2. Gale AW, Danielson DC, McGoon DC, Mair DD. Modified operation for univentricular heart and complicated congenital lesions. J Thorac Cardiovasc Surg 1979;78:831–8.
3. Kreutzer G, Galindez E, Bono H, de Palma C, Laura JP. An operation for the correction of tricuspid atresia. J Thorac Cardiovasc Surg 1973;66:613–21.
4. de Leval MR, Kilner P, Gewillig M, Bull C. Total cavopulmonary connection: a logical alternative to atriopulmonary connection for complex Fontan operations. J Thorac Cardiovasc Surg 1988;96:682–95.
5. Pearl JM, Laks H, Stein DG, Drinkwater DC, George BL, Williams RG. Total cavopulmonary anastomosis versus conventional modified Fontan procedure. Ann Thorac Surg 1991;52:180–96.
6. Laks H, Ardehali A, Grant PW, et al. Modification of the Fontan procedure: superior vena cava to left pulmonary artery connection and inferior vena cava to right pulmonary artery connection with adjustable atrial septal defect. Circulation 1995;91:2943–7.
7. Srivastava D, Preminger T, Lock JE, et al. Hepatic venous blood and the development of pulmonary arteriovenous malformations in congenital heart disease. Circulation 1995;92:1217–22.
8. Gross GJ, Jonas RA, Castaneda AR, Hanley FL, Mayer JE, Bridges ND. Maturational and hemodynamic factors predictive of increased cyanosis after bidirectional cavopulmonary anastomosis. Am J Cardiol 1994;74:705–9.
9. Salim MA, Di Sessa TG, Reed CM, Korones SB, Alpert BS. The contribution of superior vena caval flow to total cardiac output in infants: an echo-Doppler study. Clin Res 1992;17:234–41.
10. Kim YH, Walker PG, Fontaine AA, et al. Hemodynamics of the Fontan connection: an in-vitro study. J Biomech 1995;117:423–9.